Discussions on simulation models for gyrokinetic MHD: a kinetic-fluid model and a gyrokinetic PIC model (P4.150)

Y. Nishimura[1] and C. Z. Cheng

Plasma and Space Science Center, National Cheng Kung University
70101 Tainan, Taiwan

We recapitulate and discuss electromagnetic kinetic formulation which aims at simulating the effects of energetic particles on Alfvénic instabilities (Toroidicity induced Alfvén Eigenmode (TAE)[1]). The term *gyrokinetic MHD* originates from Ref.[2] which refers to recovering long wave-length magnetohydrodynamic phenomena without employing a fluid equation (but an electromagnetic gyrokinetic model). As a long term goal we also plan to simulate magnetic reconnection events in tokamaks.[3]

Two models are considered and discussed. One, a kinetic-fluid model and the other an electromagnetic gyrokinetic particle-in-cell simulation model. The kinetic-fluid model replaces the pressure evolution equation by the second order kinetic velocity moments for bulk ions, electrons, and energetic particles. As one can imagine, the two are quite similar for both the kinetics (particle pushing part) and the field equation. As a real worker who has implemented and realized the two simulation models, I would like to point out the similarity and the difference between the two.

Kinetic-fluid (KF) model[4] – To quickly illustrate, let us take a finite β reduced MHD equations:[5] the toroidal component of ideal Ohm's law,

$$\frac{\partial \psi}{\partial t} = -R^2 \left(\mathbf{v} \times \mathbf{B}\right) \cdot \nabla \zeta, \tag{1}$$

and the vorticity equation,

$$\frac{dU^\zeta}{dt} = R^2 \mathbf{B} \cdot \nabla J^\zeta + \beta \left(\nabla R^2 \times \nabla P\right) \cdot \nabla \zeta. \tag{2}$$

Here, $\mathbf{v} = R^2 \nabla \zeta \times \nabla \Phi$ is the fluid velocity, $\mathbf{U} = \nabla \times (R^2 \mathbf{v})$ is the vorticity, and $\mathbf{J} = \nabla \times \mathbf{B}$ is the current density. One can obtain shear Alfvén wave dispersion relation.[1, 6] As an exercise, let $R = 1$ in Eqs.(1) and (2) to obtain $\omega^2 = k_\parallel^2$. All the equations in this report are normalized by Alfvén frequency, major radius, and magnetic field strength at the magnetic axis. Toroidal curvature effects are included in the second term of Eq. (2).

In the KF model (the crux is), the pressure is given by (j stands for the species)

$$P_{\perp j} = \int \mu B \delta f_j d^3 v, \tag{3}$$

$$P_{\parallel j} = \int v_\parallel^2 \delta f_j d^3 v. \tag{4}$$

The second order moment of all the kinetic particles (bulk ions, electrons, and the energetic particles) from particle simulation replace the conventional pressure evolution equation.[5] The right hand sides of Eqs.(3) and (4) are gyro-averaged for the ions (thus FLR effects are present).

[1]Electronic mail: nishimura@pssc.ncku.edu.tw

The kinetic ions and electrons are given by gyrokinetic δf Vlasov equation[7]

$$\frac{\partial \delta f_j}{\partial t} = -\dot{\mathbf{X}} \cdot \nabla f_0 - \dot{v_\parallel} \frac{\partial f_0}{\partial v_\parallel}. \tag{5}$$

where

$$\dot{\mathbf{X}} = v_\parallel \frac{\mathbf{B}^\star}{B_\parallel^\star} + \bar{\omega_A} \frac{1}{B_\parallel^\star} \mathbf{b} \times (\mu \nabla B - \mathbf{E}^\star) \tag{6}$$

$$\dot{v_\parallel} = -\frac{\mathbf{B}^\star}{B_\parallel^\star} \cdot (\mu \nabla B - \mathbf{E}^\star) \tag{7}$$

are the particle position and the parallel velocity time advanced.[8] The method of characteristics is applied to incorporate Eq.(5). Here, $\bar{\omega_A} = \omega_A/\Omega_{ci}$ and $\bar{\rho_s} = \rho_s/R$.

Gyrokinetic PIC with fluid electrons – On the other hand, the fluid electron gyrokinetic model[9] by the "Fluid-kinetic hybrid electron" (FKHE) model[2] is given by[11, 12] a set of continuity equation

$$\partial_t n_e = -\nabla_\parallel u_{e\parallel}, \tag{8}$$

inverse of Faraday's law

$$\partial_t A_\parallel = \nabla_\parallel (\Phi_{eff} - \Phi), \tag{9}$$

gyrokinetic Poisson (GKP) equation

$$\bar{\omega_A} \nabla_\perp^2 \Phi = -(\delta n_i - \delta n_e), \tag{10}$$

the adiabatic relation

$$\Phi_{eff} = (\bar{\rho_s}^2/\bar{\omega_A}) \delta n_e, \tag{11}$$

and inverse of Ampere's law

$$\delta u_{\parallel e} = \bar{\omega_A} \nabla_\perp^2 A_\parallel + \delta u_{\parallel i}. \tag{12}$$

Shear Alfvén wave dispersion relation $\omega^2 = k_\parallel^2 (1 + \bar{\rho_s}^2 k_\perp^2)$ can be obtained by coupling Eqs.(8)-(12) and neglecting the kinetic ion terms. The kinetic equation (the particle pusher) is identical[3] with the KF model except that the electron gyrokinetic equation is solved only for the nonadiabatic electrons in the FKHE model. The kinetic Alfvén wave is inherent in the system due to the $\nabla_\perp^2$ operator in the gyrokinetic Poisson equation, Eq.(10). It is also found that[11] the dominant toroidal effect (which then induces TAE) is in the left hand side of Eq.(10).

Analogy of the two models – The field equations are quite similar. Note the correspondence of Eq.(1) $\rightarrow$ (9) and Eq.(2) $\rightarrow$ (10). What differentiate Refs.[9, 10, 11, 12] from other electromagnetic gyrokinetic simulation methods[15, 16, 17] is the inversion of the Faraday's law (solve the vector potential $A_\parallel$ as a dynamical equation), where conventionally Ampere's law is employed by gathering both the kinetic ion and kinetic electron currents. With the knowledge of Ohm's law, Eq.(1), the inversion can be hinted

[2] As in "kinetic-fluid model",[4] we adhere to the nomenclature in Ref.[10].

[3] All the components of the simulation code is developed independently from Refs.[11, 12]. See Refs.[13, 14] for example.

without difficulties. In the relation $E_\parallel = -\nabla_\parallel \Phi - \partial_t A_\parallel$, the parallel electric field $E_\parallel$ is imposed to be in a potential form $-\nabla_\parallel \Phi_{eff}$. To close the system for the unknown quantity Φ_{eff} , Boltzmann relation (electrons being adiabatic) is employed. As a consequence $k_\parallel = 0$ component in Eq.(9) is dropped in FKHE.[4] The collisionless reconnection is absent in the current form. Note that Eq.(1) is a projection in a toroidal angle based on the geometrical expansion,[5] while Eq.(9) is a projection onto the direction of the magnetic field lines (adiabatic electrons cannot be imposed, otherwise). The electron inertia, the Hall term, and the diamagnetic drifts due to the multi-ion-species enter the KF model through the generalized Ohm's law.[4]

On the other hand, taking a time derivative of Poisson equation gives rise to the vorticity equation [let $\delta n_i = 0$, $\delta u_{\parallel i} = 0$ and substitute Eqs.(8) and (12)]. Note that $U^\zeta \sim \nabla_\perp^2 \Phi$. We also remind that just as we solve gyrokinetic Poisson equation for each time step (in the PIC simulation), we invert the matrix $\nabla_\perp^2 \Phi$ in the MHD simulation. Strictly speaking, $\nabla_\perp^2 \Phi$ in the GKP represents polarization, however. Fluid equations in Refs.[4, 5] are derived by taking the moment of Vlasov equation. By reformulating KF model with the gyro-fluid approach[20] we can indeed incorporate polarization[21] and drift wave turbulence effects.

While the gyrokinetic PIC simulation includes all the waves under cyclotron frequency, in the kinetic-fluid model, we incorporate wave dynamics one by one (and confirming each piece of wave dynamics). For example, by adding parallel velocity equation to Eq.(1) and (2), one can see the coupling of sound wave and shear Alfvén wave.[22] The kinetic Alfvén wave is absent in the MHD equation unless we incorporate Eqs.(3) and (4).

Simulation results – We present our preliminary numerical simulation results by the kinetic-fluid model. In Ref.[23], Alfvén wave propagation in a cylinder and the generation of the TAE frequency gap in a torus are demonstrated employing the kinetic-fluid model. Compared to the majority of the kinetic-MHD hybrid simulation[24, 25, 26, 27, 28] the present work is unique in that it incorporates bulk kinetic ions and electrons.

Parameters used are similar to those of burning tokamak plasmas,[29] $R = 5.00(m)$, $a = 1.25(m)$, $B_0 = 4.3(T)$, $T_i = T_e = 10.0keV$, $n_0 = 1.0 \times 10^{20}(m^{-3})$. We have taken multi species ions (deuterium, tritium, and energetic particles) and electrons. The energetic particles are given by Gaussian distribution with the thermal velocity set to the Alfvén velocity. Note that at the moment, the numbers of marker particles are *not* proportional to the background density (as a reminder we employ δf method), due to the limited numbers of processors [16 nodes ($\times 4$)] at our local Linux cluster.

The TAE mode is excited in the presence of energetic particle ions. Linear modes of $m/n = 1/1$ and $m/n = 2/1$ are present in the system. The mode amplitudes of the fluctuation experience an exponential growth of the envelope together with the oscillation at the TAE frequency. In Fig.1(a), the TAE eigenmode structure in the presence of the energetic particles is shown. In Fig.1(b) the linear growth rate versus the β_α is shown in the absence and in the presence of the kinetic (bulk) ions and electrons. Here, $\beta_\alpha = 4\pi p_\alpha / B_0^2$ (p_α is the pressure of the energetic particles). For the TAE excitation in the gyrokinetic particle simulation, see Ref.[12].

[4]The zonal component of the vector potential can be obtained by taking a flux surface average of the Ampere's law.[18, 19]

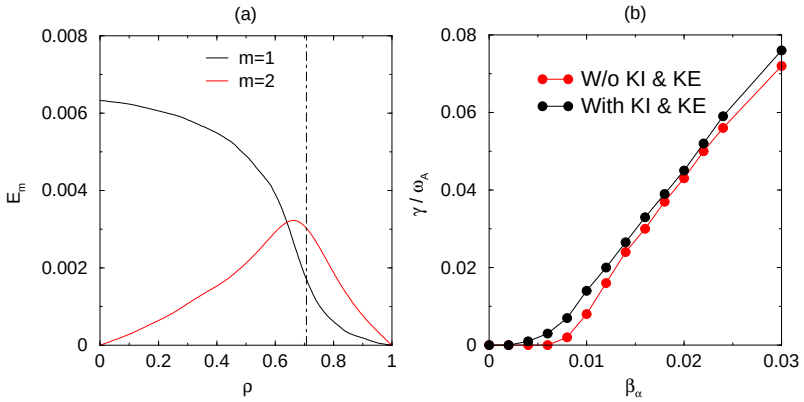

Figure 1: (a) The TAE eigenmode structure in the presence of the energetic particles. (b) The linear growth rate versus the β_α in the absence and in the presence of the kinetic (bulk) ions and electrons. The slow onset at low beta region is due to the sensitivity to the number of marker particles. In the case with the bulk ions and electrons, the Alfvénic instabilities do get excited at the smaller values of β_α , however.

This work is supported by National Cheng Kung University Top University Project. The authors thank for recent discussions with B. Scott, N. Gorelenkov, and H. Park.

References

[1] C. Z. Cheng and M. S. Chance, Phys. Fluids **29**, 3695 (1986).
[2] H. Naitou *et al.*, Phys. Plasmas **2**, 4257 (1995).
[3] Y. Nishimura, J. D. Callen, and C. C. Hegna, Phys. Plasmas **6**, 4685 (1999).
[4] C. Z. Cheng and J. R. Johnson, J. Geophys. Res. **104**, 413 (1999);
[5] H. R. Strauss, Phys. Fluids **20**, 1354 (1977).
[6] G. Y. Fu and J. W. Van Dam, Phys. Fluids B **1**, 1949 (1989).
[7] A. M. Dimits and W. W. Lee, J. Comput. Phys. **107**, 309 (1993).
[8] R. G. Littlejohn, J. Plasma Phys. **29**, 111 (1983).
[9] S. E. Parker, Y. Chen, and C. Kim, Comput. Phys. Comm. **127**, 59 (2000).
[10] Z. Lin and L. Chen, Phys. Plasmas **8**, 1447 (2001).
[11] Y. Nishimura, Z. Lin and W. X. Wang, Phys. Plasmas **14**, 042503 (2007).
[12] Y. Nishimura, Phys. Plasmas **16**, 030702 (2009).
[13] Y. Nishimura, Y. Xiao, and Z. Lin, Contrib. Plasma Phys. **48**, 224 (2008).
[14] Y. Nishimura, submitted to Comput. Phys. Comm. (2010).
[15] W. W. Lee *et al.*, Phys. Plasmas **8**, 4435 (2001).
[16] Y. Chen and S. E. Parker, Phys. Plasmas **8**, 2095 (2001).
[17] A. Mishchenko, R. Hatzky, and A. Könies, Phys. Plasmas **11**, 5480 (2004).
[18] M. N. Rosenbluth, F. L. Hinton, and Z. Lin (private communication 2003).
[19] Y. Nishimura *et al.*, Bull. Am. Phys. Soc. **48**, LP1.060 (2003).
[20] A. J. Brizard, Phys. Fluids B **4**, 1213 (1992).
[21] W. W. Lee, J. Comput. Phys. **72**, 243 (1987).
[22] M. Yagi and N. Nakajima (private communication 2009).
[23] Y. Nishimura and C. Z. Cheng, J. Plasmas and Fusion Res. Series **9**, (2010).
[24] C. Z. Cheng, J. Geophys. Res. **96**, 21159 (1991).
[25] W. Park *et al.*, Phys. Fluids B **4**, 2033 (1992).
[26] G. Y. Fu and W. Park, Phys. Rev. Lett. **74**, 1594 (1995).
[27] S. Briguglio *et al.*, Phys. Plasmas **2**, 3711 (1995).
[28] Y. Todo and T. Sato, Phys. Plasmas **5**, 1321 (1998).
[29] ITER Physics Expert Group on Energetic Particles, Nucl. Fusion **39**, 2471 (1999).